Studies on Kinetics, Isothermal Modelling and Optimization of Cow Dung Adsorbent for Synthetic Dairy Wastewater Treatment

Anitha. A.S[1,2], Dawn. S.S[3,4*], Muthukumaravel. K[2], Praveen. R[5]

[1]Department of Chemical Engineering, Sathyabama Institute of Science and Technology, Chennai – 600 119, India

[2]Department of Biotechnology, Karpaga Vinayaga College of Engineering and Technology, Chengalpattu – 603 308, India

[3]Centre for Waste Management, Sathyabama Institute of Science and Technology, Chennai – 600 119, India

[4]Centre of Excellence for Energy Research, Sathyabama Institute of Science and Technology, Chennai – 600 119, India

[5]Research & Development, Cornerstone Additive Manufacturing Solutions Private Limited, Chennai – 600 117, India

[*]Corresponding author: Dr. S.S. Dawn

E-mail: dawn@sathyabama.ac.in , tel: +91-98409 96791

GRAPHICAL ABSTRACT

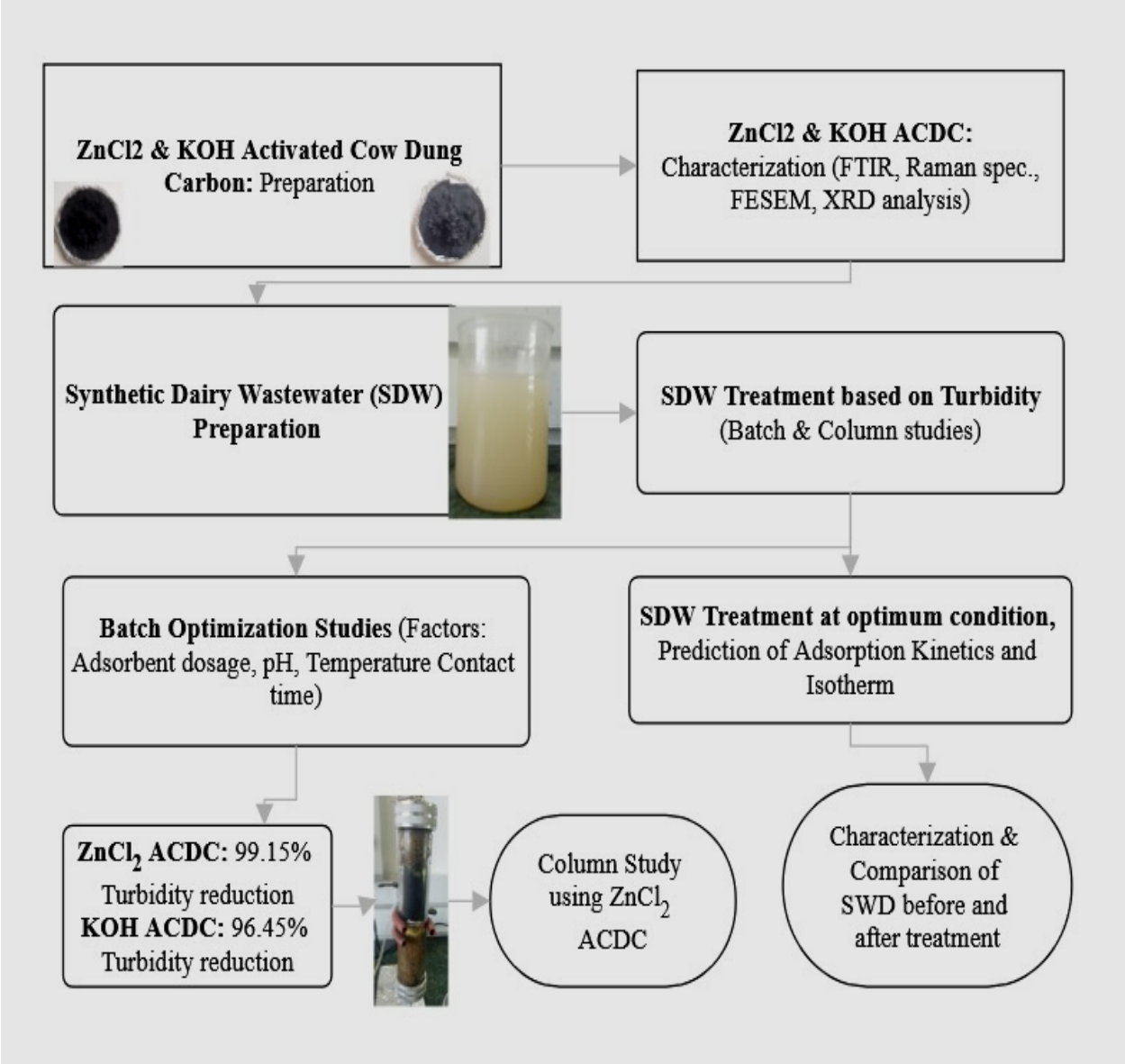

ABSTRACT

The dairy industry is a major food industry that processes raw milk into a variety of products. The milk processing factory produces DWE with soluble organic components, suspended particles, and trace elements. These components degrade, causing cloudiness and odour. Adsorbing total solids (TS) and controlling odour levels in dairy wastewater help to minimize odour. This study investigates the process of producing activated carbon from cow dung (ACDC) and its use in cleaning synthetic dairy wastewater (SDW) by batch adsorption and column adsorption studies. Cow dung powder is chemically activated by soaking it in 1N $ZnCl_2$ and 1N KOH solutions in a 2:1 ratio. The optimal adsorbent concentration for both ACDC was 2.5 g/50 ml. The effectiveness of ACDC treatment was evaluated by its ability to reduce turbidity, TDS, and COD. The study found that activated carbon with $ZnCl_2$ was slightly more effective than activated carbon with KOH. While the KOH ACDC was more effective at a pH of 8, achieving a removal rate of 92.88%, the $ZnCl_2$ ACDC achieved a turbidity removal of 93.3% at a pH of 4. The present work highlights the potential for activated carbon derived from cow dung to effectively and sustainably treat dairy effluent.

Keywords: Activated Carbon, Adsorption Kinetics, Adsorption Isotherms, Fixed Bed Column, Odour, Synthetic Dairy Wastewater, Turbidity

1. INTRODUCTION

Rapid increase in world's population has an impact on the number of food industries available. Dairy industry is most important among them. Such increasing population impose an increasing demand on the availability of food including milk, which tremendously increases the production rate of milk and other products (Luo & Ding, 2011). The dairy industry packs and processes raw milk into products such as butter, curd, cheese, and dried milk powder by various process including chilling, pasteurization, fermentation, homogenization and so on. After milk processing and product packing, the vessels involved in the process are washed with washing detergents and chemicals along with water collectively known as wash water (Santos et al., 2020). Dairy wastewater is generated from several process points, including receiving point, canning plant, milk processing plant, and other products producing plants which varies based on industries location. Dairy wastewater contains high amounts of organic content, lactose sugar, casein and other proteins, detergents, sanitizing agents, dirt, etc., (Luo & Ding, 2011). In 2022, world's total milk production had reached 935.9 million tons and reached 944.0 million tons in the year 2023 resulting in a 0.9 % increase from previous year (FAO, 2023). India ranks 1st globally in milk production as per economic survey 2022-23, India produced 230.58 million tons of milk, accounting for 24.64% of world output in the year 2021-22. India's per capita milk availability increased from 407 g/day in 2019-20 to 459 g/day in 2022-2023 (DAHD&F, 2023). Dairy industries generate an average of 4L - 15 L of wastewater effluent for 1 litter of processed product and are released into nearby water sources, which places them among the most polluting industries (Santos et al., 2020). Dairy industry wastewater poses a serious environmental problem due to presence of rich organic content (Shete & Shinkar, 2013). Around 4 - 11 million tonnes of dairy wastewater are discharged into the environment annually, posing threat to the

ecosystem (Ahmad et al., 2019). Direct discharge of untreated dairy wastewater into nearby water bodies can lead to increasing dissolved oxygen demand which are caused by fat effluents including oil and grease content creating a film on the water's surface, preventing oxygen transport and making it difficult for aquatic creatures and hydrophytes to survive (Ahmad et al., 2019; Rosa et al., 2009). Due to the presence of suspended solids, dissolved solids, lactose, organic components, nutrients (like K, N, P, etc.), lipids, sulphates, chlorides and so on., the dairy wastewater effluent has a high Biological Oxygen Demand and Chemical Oxygen Demand. Dairy effluent has BOD (40 - 48,000 mg/L) and COD (80 - 95,000 mg/L) content approximately, and pH varies between the range of 4.7 - 11 based on the decomposition of milk sugars and nature of cleaning water used, which may contain various sterilizing agents and washing detergents (Ahmad et al., 2019). According to Slavov (2017) and Shete & Shinkar (2013), dairy wastewater effluent is turbid which has whitish - yellow appearance and has an unpleasant odour. Cheese waste contains excess suspended particles due to presence of fine curd. Since, the dairy industry mainly relies on water makes it challenging to safely dispose of considerable amounts of effluent (Yonar et al., 2018). Dairy wastewater has high organic content which supports the growth of anaerobic bacteria which causes unpleasant odour, affecting the air quality causing breathing uneasy. The turbidity of the solution will be high in wastewater producing unpleasant odour and are known as secondary indicator of odour (Mucha & Kułakowski, 2016). In order to preserve environmental quality, dairy effluent should be treated prior to discharge in nearby water bodies (Muniz et al., 2020)

Dairy wastewater is often treated based on both physicochemical and biological approaches. Various techniques including coagulation and oxidation are used to remove COD from wastewater. They are effective in terms of time but requires huge investment, power supply,

chemical detergent usage, and enough space for the process (Pathak et al., 2016). The biological treatment application is increasing widely due to its lower cost and higher efficiency, but it's a time-consuming process (Ahmad et al., 2019). Adsorption is a promising technology for organic content reduction by the means of time, economy and easy process operation. Bio-sorption is the process involves removal of solute molecules from solvent by using a cheap adsorbent with high availability. Bio-sorbents are mostly activated carbon prepared from agricultural and animal waste including maize cobs, corn stalk, rice husk, cassava peel, vegetable waste, grill manure, cow dung and so on, which have been recently explored as new path resulting in an alternative and effective approach for bio based activated carbon production (Pathak et al., 2016). Activated carbon with large surface area and pore size is commonly employed in industrial applications such as solute extraction, bio-glycerol purification, solvent recovery, and water treatment (Demiral & Demiral, 2008). Since, the dairy industry depends upon heard of cows for milk production, resulting in accumulation of huge quantity of waste after the digestion of food the cattle are fed with. Cow dung is commonly utilised as home fuel in some rural areas, used to prepare manure and are disposed of without any consideration which attracts the consideration of pollution prevention (Demiral & Demiral, 2008). Cow dung consists of 14% hemi-cellulose content, 15% cellulose content, and 7% lignin content. This property supports the use of cow dung's potential as an activated carbon precursor. Carbon consumption determines the activated carbon's surface area and pore size. However, cow dung based activated carbon has a considerable impact yield (Park et al., 2022). Demiral and Demiral (2008), have successfully synthesized activated carbon from cow dung using $ZnCl_2$ and KOH solution found to be having larger surface area. This study aims to examine the potential of Activated Cow Dung Carbon (ACDC) as a bio-sorbent for removal of organic contaminants from synthetic dairy wastewater

and its characteristics through batch optimization studies and to perform column study for both ACDC.

2. MATERIALS AND METHODS

2.1. Activated Carbon Preparation

For this study the cow dung was chosen as precursor material in preparation of activated carbon. The precursor material is sun dried for a week and then dried at 105 °C for 3 hours to remove excess moisture content with the help of hot air oven. The dried precursor material is crushed using a mixer grinder followed by sieve analysis using sieve of mesh size 80 to get fine particle of uniform size (~177 µm). Chemical activation of powdered precursor material was carried out using 1N $ZnCl_2$ and 1N KOH solution (Demiral & Demiral, 2008). Chemical activation process was carried out by impregnating the precursor material with $ZnCl_2$ and KOH solution at a ratio of 2:1 (2ml/g of precursor material) for approximately 2 hours at 80 °C to obtain a homogenous slurry. The homogenous slurry was then dried at 105 °C for 2 hours before pyrolysis process. After drying, the material was carbonised using a Muffle furnace at 500 °C in a closed crucible for an hour. Then, the activated carbon was washed with distilled water to remove excess chemicals used for activation and to deduce the pH around pH 7 - 8. Prepared ACDC was dried at 105 °C for 2 hours to remove moisture content and stored in an airtight container for future use.

2.2. Synthetic Dairy Wastewater Preparation

Synthetic Dairy Wastewater (SDW) was prepared using commercially available milk powder, for this study Britannia milk powder, glucose, certain salts used in washing, the SDW composition is designed as such to stimulate normal dairy wastewater effluent by mimicking its features. SDW was prepared similar to those that in earlier publications (Healy et al., 2007; Fdegaard & Rusten,

1980). SDW was freshly prepared everyday by the composition as given in Table 1. The SDW composition remained consistent throughout the experiment and was made fresh as needed. The SDW samples subjected to standard parameter tests including pH, TDS, TSS, turbidity, BOD, and COD, electrical conductivity, alkalinity test, salinity test, and chloride test using standard procedures.

Table 1. Composition of SDW

S. No.	Component	Amount (mg/L)
1	Dried Milk	1440
2	Glucose	2400
3	Yeast	300
4	$CO(NH_2)_2$	270
5	$NaHCO_3$	1560
6	$KHCO_3$	600
7	NH_4Cl	580
8	$Na_2PO_4.12H_2O$	900
9	$MgSO_4.7H_2O$	600
10	$MnSO_4.H_2O$	24
11	$FeSO_4.7H_2O$	24
12	$CaCl_2.6H_2O$	36
13	Bentonite	488

2.3. Experimental Batch Study:

The batch adsorption studies were carried out with the help of incubator shaker using 250 mL glass-stopper conical flasks with varying operating conditions. The pH of prepared SDW was changed between acidic and basic as necessary using HCl (0.1 N) and NaOH (0.1 N) solutions and the pH of SDW was determined using a digital pH metre. A known quantity of ACDC was added to 50 ml sample and agitated at 150 rpm for 20mins at 30 °C for adsorption process to be carried out. The mixtures were then filtered by the means of filter paper (Pathak et al., 2016). The final turbidity in the filtrate was measured using a nephelometer (Ramya et al., 2021). The effect of operating condition on percent removal of turbidity by ACDC was observed by varying the parameters including adsorbent dosage (0.5, 1.0, 1.5, 2.0, 2.5 and 3 g /50 ml), followed by pH of SDW (2, 4, 6, 8, and 10), temperature (303K, 308 K, 313 K and 318 K), and reaction time (10, 15, 20, 25 and 30 mins), were studied to determine their impact on removal percentage (Pathak et al., 2016). The adsorption capacity of prepared ACDC was measured using the following equation 1.

$$q_e = \frac{(C_i - C_e)}{m} \times V \qquad \ldots (1)$$

Where, C_i is the initial concentration, C_e is the final concentration, V is the volume of SDW, m is the mass of the adsorbent.

By using the optimum conditions obtained from the batch studies, the prepared SDW treated using both the ACDC at peak conditions to provide optimum result. The treated water was then subjected to characterization test including pH, chlorides, TDS, TSS, electrical conductivity, COD, BOD, alkalinity, hardness and turbidity and it was compared against to that of the parameters of untreated SDW. ACDC after adsorption at optimum conditions were subject through surface characterization test including FTIR, SEM, and Raman spectroscopy.

2.4. Experimental column Studies

Using the optimum conditions obtained from the batch studies, the continuous column study was carried out using a fixed bed column (Kulkarni et al., 2022). The column used for this study was 21cm in height and 10 cm in diameter. The column is packed with $ZnCl_2$ activated carbon of height 5cm and the adsorbent layer is sandwiched between sand (6 cm each) on both sides to maintain a constant flow of SDW throughout the column. The layers of the column were then stabilized by placing sponge between each layer and then with mesh and both ends to prevent the escape of packing materials. The column experiment was carried with a constant flow rate of 5 ml/min.

3. RESULT AND DISCUSSION

3.1. BATCH ADSORPTION STUDY

Effect of adsorbent dosage: The experimental study was carried out with constant temperature of 30°C, agitation speed of 150 rpm, adsorption time of 20 mins, pH of 7.38, and varying adsorbent quantity (0.5, 1.0, 1.5, 2.0, 2.5, and 3 g/50ml). For ZnCl2 treated ACDC, the percent removal of turbidity increased significantly as the dosage increased up to 2.5g (93.3%) and when 3g of adsorbent used, there is a slight decrease in percent removal of turbidity (81%). Figure 1(a) shows graph of percent removal of turbidity based on adsorbent dosage. In the case of KOH activated ACDC, the percent removal of turbidity increased significantly as the dosage increased up to 2.5g (92.88%) and when 3g of adsorbent used, there is a slight decrease in percent removal of turbidity (89.49%). Figure 1(a) shows graph of percent removal of turbidity based on adsorbent dosage. Considering every other parameter, the first dosage showing good reduction percent (1g/50ml) which has given 88.8% reduction by $ZnCl_2$ ACDC treatment and 88.9% reduction by KOH ACDC treatment has been chosen for all the further studies.

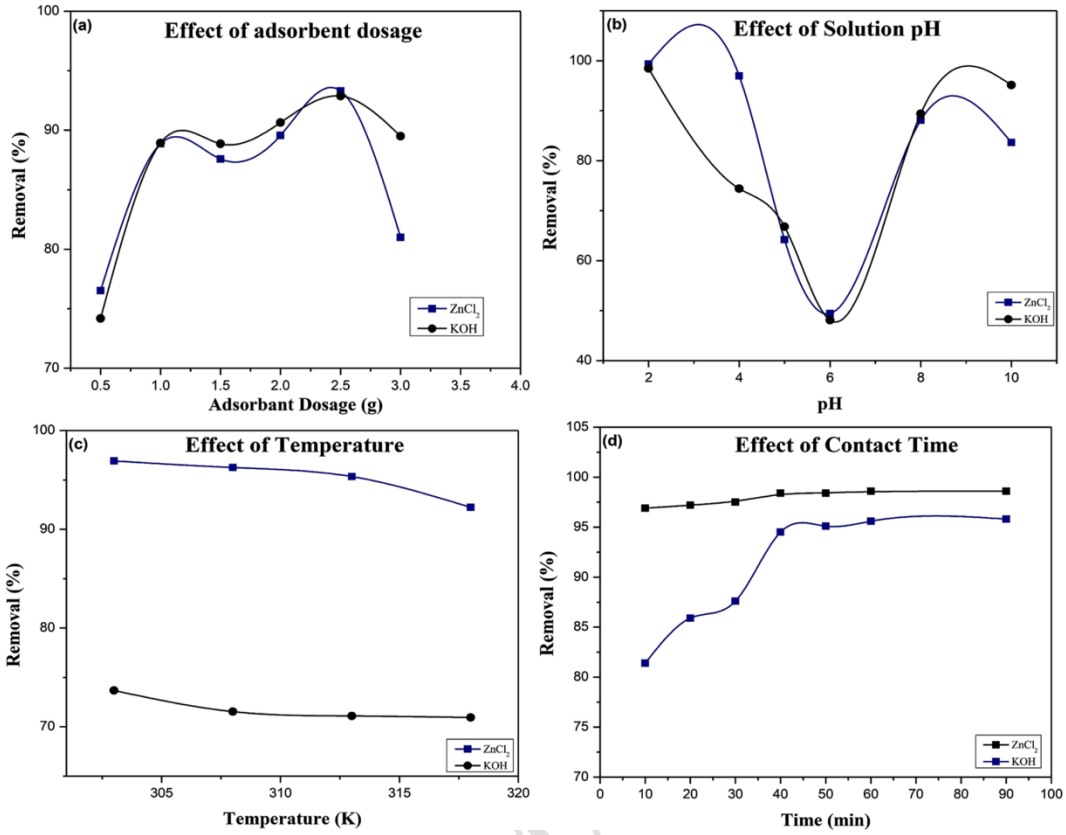

Figure 1. (a) Adsorbent Dosage optimization graph for both ACDC (b) pH optimization graph for both ACDC (c) Temperature optimization graph for both ACDC and (d) Time optimization graph for both ACDC

Effect of pH: In the bio-sorption studies, pH of the solution is the important factor which strongly influences the odour dairy effluent (Tikariha & Sahu, 2014) and also plays a key role in the determination of efficiency of the treatment process using ACDC. The adsorbent's surface charge, organic substance ionization, and functional group dissociation on active sites are influenced by the pH of solution. In this process, pH of SDW was altered from the range of 2 to 10 (used for treatment using both the prepared ACDC) ranging from highly acidic to alkaline condition by keeping the rest of the parameter constant (adsorbent dose of 1g/50ml, temperature of 30 °C, and agitating speed of 150 rpm and contact time of 20 mins). From Figure 1(b), it is shown that at lower pH, the effect of ACDC treatment increased for both ACDC in the terms of

turbidity reduction, as the pH increased towards neutral the efficiency of treatment decreased significantly and in the case of KOH it showed better treatment efficiency in the higher pH (pH 10), but having a major drawback i.e., the pH of the treated water is around. 8 – 8.5. Based on these considerations, the temperature optimization process was carried out with pH 4 for the $ZnCl_2$ ACDC and pH 8 is for the KOH ACDC treatment process.

Effect of temperature: From Figure 1(c), the temperature affects the adsorption process while keeping other parameter such as adsorbent dose of 1g/50ml, pH 4 (for ZnCl2 ACDC) & pH 8 (for KOH ACDC), contact time of 20 mins and agitation speed of 150rpm). Temperature was changed between 30 °C and 45 °C. The percent reduction of turbidity gradually reduced as the temperature increases. This may be due to the bonds between the adsorbate molecules and the ACDC binding site weaken as the temperature increases (for both the activated carbons), resulting in decreased binding capability (Pathak et al., 2016). As the temperature of the operating condition drops, organic molecules are more likely to be absorbed due to the spontaneous nature of the process.

Effect of contact time: The contact time is another factor which has significant effect on the removal efficiency. As the contact time increases the removal efficiency increases. For this study, the contact time is increased from 10 mins to 60 mins with an interval of 10 mins each and the process is extended up to 90 mins to obtain the equilibrium concentration of the adsorbate. Figure 1(d) represents the effect of contact time. In the case of KOH ACDC at time of 40 mins the removal percent reaches its mere maximum. In the case of $ZnCl_2$ the removal percent of turbidity is effective even at 10 mins showing its efficiency at treating the SDW and from 40 mins there is no significant change found in the percent removal till 90 mins.

3.2. ADSORPTION ISOTHERM

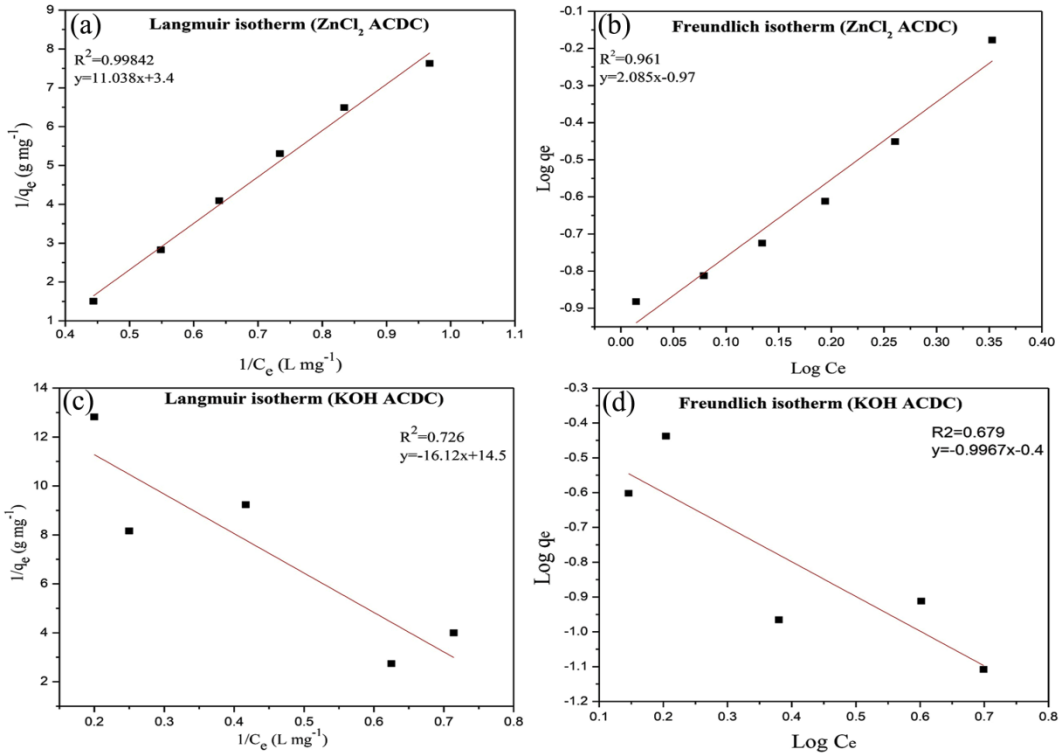

Figure 2. (a) Langmuir isotherm of $ZnCl_2$ ACDC (b) Freundlich isotherm of $ZnCl_2$ ACDC (c) Langmuir isotherm of KOH ACDC and (d) Freundlich isotherm of KOH ACDC

Langmuir and Freundlich isotherm models were used for understanding the adsorption process and theoretical prediction for this study. The Langmuir isotherm is recognized as the most commonly used adsorption model. Irving Langmuir (1916), an American scientist, formulated this theoretical isotherm to characterize adsorption on activated carbon (Chowdhury et al., 2011). The Langmuir isotherm implies monolayer adsorption onto a surface considering no interaction between adsorbed molecules, whereas the Freundlich isotherm permits multilayer adsorption with interactions between adsorbed molecules. The Langmuir and Freundlich equations (2) and (3) are as follows:

$$\frac{1}{q_e} = \left(\frac{1}{K_L q_m}\right)\frac{1}{C_e} + \frac{1}{q_m} \quad \ldots (2)$$

$$logq_e = logk_f + \frac{1}{n} lnC_e \quad \ldots (3)$$

Where, equation 2 - Langmuir equation and equation 3 - Freundlich equation K_L (mg^{-1}) is Langmuir constant, K_f ((mg/g) $(dm^3/mg)^{1/n}$) is Freundlich constant, C_e is the equilibrium concentration of adsorbate (mg/L), n is adsorption intensity and q_e is the amount of the adsorbate adsorbed by the adsorbents at equilibrium (mg/g).

Adsorption isotherm for $ZnCl_2$ ACDC: K_L and q_m of adsorption process was determined using the slope and intercept of the plot between $1/C_e$ vs $1/q_e$ which is shown in Figure 2(a). The Freundlich isotherm graph (Log C_e vs Log q_e) for the Zinc chloride activated cow dung carbon is given in Figure 2(b). From these graphs we can infer that the Langmuir isotherm graph has R^2 value of 0.998 and the Freundlich isotherm graph has R^2 value of 0.961, suggesting the fitness of Langmuir isotherm model for this study showing a maximum adsorption capacity of 0.3 mg/g. Isotherm parameters are given in Table 2.

Table 2. Adsorption isotherm parameters of ZnCl2 ACDC & KOH ACDC

Parameters	**$ZnCl_2$ ACDC**	**KOH ACDC**
Intercept	-3.4395	14.502
Slope	11.0556	-16.113
K_L	-0.3111	-0.8997
q_m	0.29411	0.0689
R^2	0.99784	0.7263
Intercept	-0.9696	-0.4
Slope	2.0849	-0.9967
K_f	0.3792	0.6703

1/n	2.085	-0.9967
R^2	0.9614	0.6797

Adsorption isotherm for KOH ACDC: From Figures 2(c) & 2(d), we can also understand that the coefficient of determination R^2 value of Langmuir isotherm and Freundlich isotherm for KOH activated cow dung carbon is 0.72 & 0.689 respectively suggesting that the Langmuir isotherm model is the best fitting and most suitable isotherm model for KOH ACDC showing a maximum adsorption capacity of 0.07mg/g. From Figure 2(d), Freundlich isotherm model, a slope value of -0.9967 denotes a significantly inverse relationship between $\log q_e \; and \; \log C_e$ implying that the amount of solute adsorbed by the adsorbant rapidly decreases as the adsorbate concentration increases. It suggests that the saturation of adsorption sites or other variables influencing the adsorbent's adsorption capability may prevent the adsorption process from favoring larger concentrations showing a significant negative correlation between concentration and adsorption, indicating a somewhat less dramatic drop in adsorption with increasing solute concentration.

3.3. ADSOROTION KINETICS:

Experimental data was tested against pseudo first-order and second-order equations to understand the adsorption mechanism (Özcan & Özcan, 2004). According to pseudo 1st order kinetic model, the difference between the amount of adsorbate adsorbed at any given time (t) and the equilibrium adsorption capacity (q_e) determines the rate of adsorption (Stanly et al., 2020).

$$\ln(q_e - q_t) = lnq_e - \; k_1 t \qquad \ldots (4)$$

Pseudo first & second order kinetic expression is given below respectively.

Here, $slope = \; k_1 t$ and = Intercept = lnq_e

$$\frac{t}{q} = \frac{1}{k_2 q_e^2} + \frac{t}{q_e} \quad \ldots (5)$$

Here, $slope = \frac{1}{q_e}$ and $\text{Intercept} = \frac{1}{k_2 q_e^2}$

where q_e and q_t are the amounts of adsorbate adsorbed onto adsorbent at equilibrium and at t (min) respectively, and k_1 (min^{-1}) & k_2 (g mg^{-1} min^{-1}) is the rate constant of first & second order kinetics respectively. From graph $\log(q_e - q_t)$ vs t, k_1 and q_e can be estimated based on their intercept and slope for first order kinetics, from graph t/q_t vs t, k_2 and q_e can be estimated based on their intercept and slope for second order kinetics.

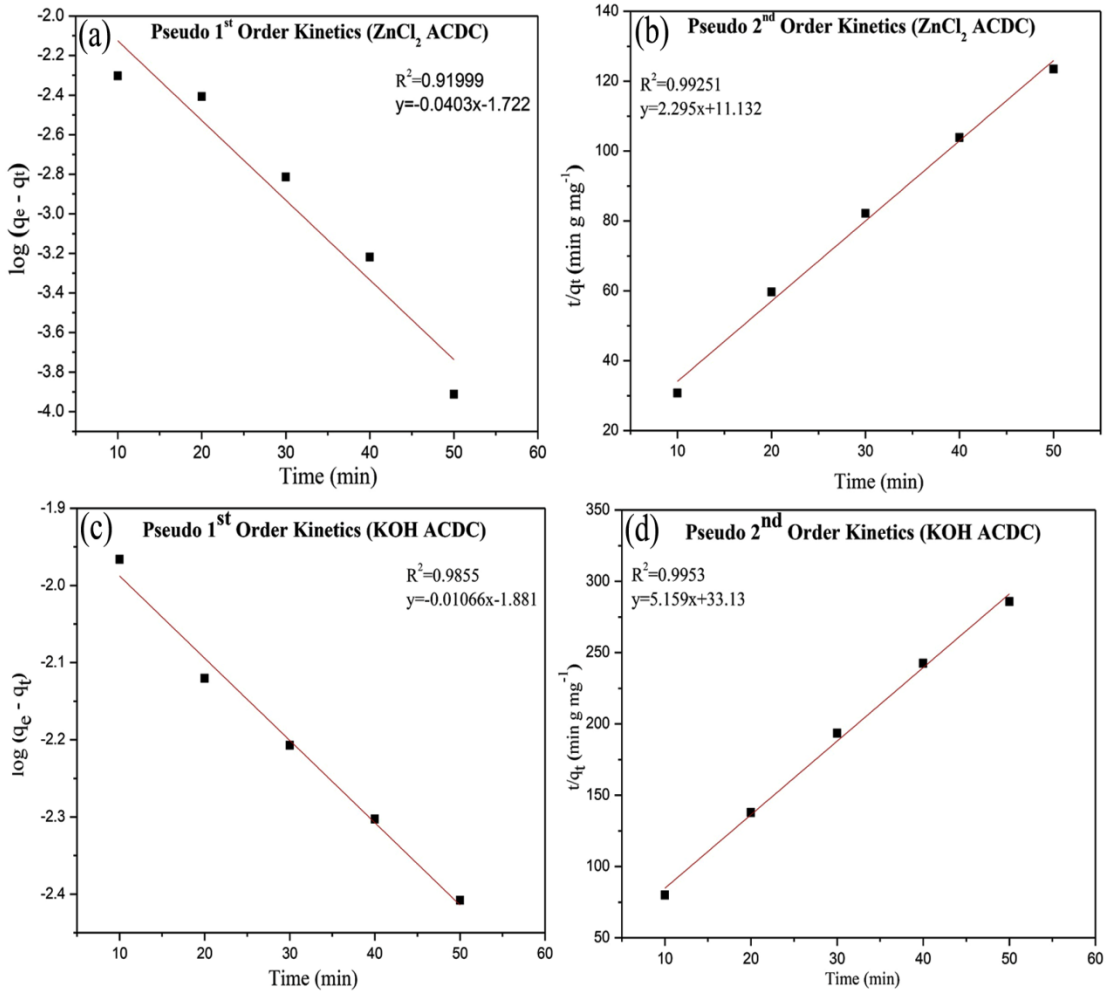

Figure 3. (a) Pseudo 1st order kinetics of $ZnCl_2$ ACDC (b) Pseudo 2st order kinetics of $ZnCl_2$

ACDC (c) Pseudo 1st order kinetics of KOH ACDC and (d) Pseudo 2nd order kinetics of KOH ACDC

Adsorption Kinetics of $ZnCl_2$ ACDC: Figure 3(a) describes the graph of log (q_e - q_t) vs time, by using the intercept and slope of the graph, the theoretical q_e and rate constant k_1 value are predicated respectively. The pseudo 1st order kinetic plot interprets the R^2 value of 0.919. The equilibrium adsorption capacity (q_e) predicted by the pseudo 1st order kinetic model is 0.178 mg/g. Figure 3(b) describes the graph of pseudo 2nd order kinetic plot of $ZnCl_2$ ACDC, which interprets the R^2 value of 0.99251 and the q_e predicted by the pseudo 2nd order kinetic model is 0.44 mg/g similar to that of experimental data. The high value of R^2 suggests that the pseudo 2nd order kinetic model closely represents the adsorption process and effectively captures the relationship between adsorbate concentration and adsorption rate.

Adsorption Kinetics of KOH ACDC: Figure 3(c) represents pseudo 1st order kinetics which interprets the R^2 value of 0.985. q_e predicted by the pseudo 1st order kinetic model is 0.15 mg/g. Fig 3(d) describes the graph of t/q_t vs time, by using the intercept and slope of the graph the theoretical q_e and rate constant k_2 value are predicated respectively. The pseudo 2nd order kinetic plot interprets the R^2 value of 0.995 and q_e predicted by the pseudo 1st order kinetic model is 0.194 mg/g. The high value of R^2 suggests that the pseudo 2nd order kinetic model likely represents the adsorption process and effectively captures the relationship between adsorbate concentration and adsorption rate.

3.4. SYNTHETIC DAIRY WASTEWATER CHARACTERISTICS

The parameters of untreated SDW compared to the parameters of SDW treated with ZnCl2 ACDC and KOH ACDC as shown in the Table 3. This table clearly shows the efficiency of both the activated carbons in the treatment of SDW, both the activated carbons show a significant

reduction in the parameters of SDW including turbidity, TDS, salinity, hardness, BOD, COD, along with the pH control (almost neutral). Based on the performance of both the activated carbons, the ZnCl2 ACDC show a higher reduction of parameters when compared to the KOH ACDC. The Chlorine content of ZnCl2 ACDC treated SDW seem to be higher due to the nature of the activation chemical used.

Table 3. Parameter analysis of synthetic dairy water with before and after ZnCl2 and KOH ACDC treatment at optimum condition

Parameter	**Synthetic Wastewater (Untreated)**	**Zncl$_2$ -Treated Wastewater**	**KOH - Treated Wastewater**
Turbidity (NTU)	532	4.5	18.9
pH	6.78	7.1	7.46
TDS (ppm)	1870	1230	1490
Chloride content (mg/L)	536	659.6	495.8
Salinity (%)	10	6	6
Hardness(mg/L)	35	25	25
Electrical Conductivity (m)	1.55	1.00	1.352
Alkalinity (mg/L)	1740	125	1460
COD (mg/L)	500	67	75
BOD (mg/L)	270	45	57

3.5. ACTIVATED COW DUNG CARBON CHARACTERISTICS

3.5.1. Raman Spectroscopy

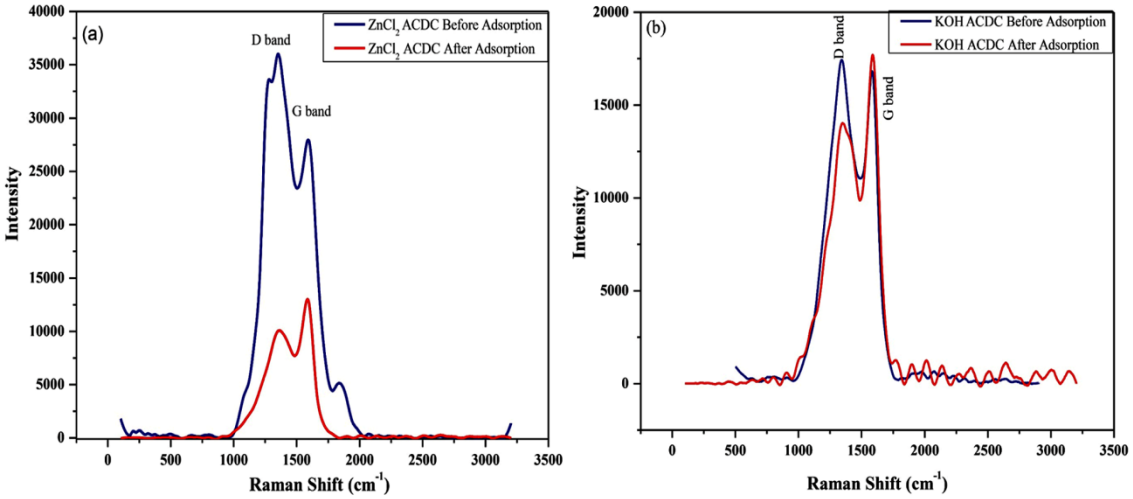

Figure 4. (a) Raman spectra of $ZnCl_2$ ACDC activated carbon before and after adsorption and (b) Raman spectra of KOH ACDC activated carbon before and after adsorption

Raman spectroscopy may be used to analyze subtle structural and the modes of vibration of molecules changes in activated carbons. This characterization method is best suited for determining functionalization levels in ACDC sample and its carbon-based compounds (Liu et al., 2017). Raman spectra show two distinct rotational contributions: the G-band (graphitic nature of the carbon) to symmetric vibrations, and A_1g in-plane rotating modes (refers to anti-symmetric band at 1580 cm^{-1} and the D-band (disorder band - defects or disorder in the carbon structure) at 1355 cm^{-1}, which correspond to the E_2g (refers vibrations perpendicular to the principal axis). The position and breadth of these bands vary based on the degree of carbonization (Dubey et al., 2022). The intensity of the D band varies based on pores size and number, size of the microcrystal's, and so on (Dubey et al., 2022). The Raman spectra for the $ZnCl_2$ ACDC before and after adsorption is shown in Figure 4(a), $ZnCl_2$ ACDC before adsorption has D and G bands at 1354.8 cm^{-1} and 1589 cm^{-1}, respectively indicating the

presence of highly active sp^3 hybridized bonds. In the $ZnCl_2$ ACDC after adsorption process the intensity of the peak seems to be reduced at 1365.7 cm^{-1} of D band and 1589.6 cm^{-1} at the G band. Here, the intensity drop at D band is caused due to the accumulation of adsorbate onto its surface pores of ACDC and at G band intensity drop may be due to changing of chemical structure in surface by chemisorptions of adsorbate.

In the case of KOH ACDC, the D band has the shift from 1342.8 cm^{-1} to 1346.7 cm^{-1} indicating changes in the pore size or crystalline structure of the KOH ACDC after adsorption and the increase in the G Band Intensity, attributes to an increase in the ordered carbon domains after adsorption process. Considering the intensity of the D band and G band formed in KOH & $ZnCl_2$ ACDC before adsorption, we can say that the $ZnCl_2$ activation has created more macropores than the KOH activation of cow dung carbon.

3.5.2. FTIR Analysis

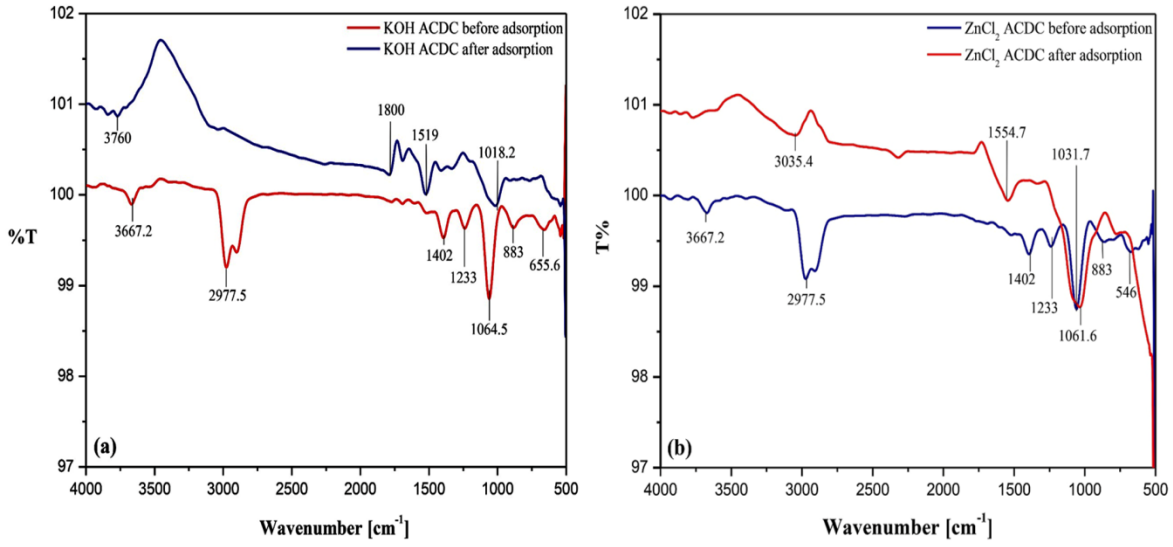

Figure 5. (a) FTIR of ACDC KOH activated carbon before and after adsorption and (b) FTIR of ACDC $ZnCl_2$ activated carbon before and after adsorption

The FT-IR band spectra of the ACDC before adsorption process shows some functional groups as shown in Figure 5. The FTIR spectra of KOH & $ZnCl_2$ ACDC spectra were obtained using

FT/IR-6600 type A spectrometer in the wave range of 500-4000 cm^{-1}. The spectra of both the KOH & $ZnCl_2$ ACDC before adsorption were found to be similar indicating that the activation process using the KOH & $ZnCl_2$ chemicals doesn't change the surface functional groups of the CD. ACDC's surface chemical characteristics and pore structure has a significant impact on adsorption capability. Analyzing functional groups on the surface of both ACDC before and after adsorption may show changes in surface chemical characteristics.

The ACDC had more organic elements, resulting in more functional groups. The ACDC showed band for OH-bounded groups of phenols and alcohols (3667.2 cm^{-1}), strong double peak of alkanes stretching vibration at 2977.5 cm^{-1}(C-H), a strong narrow peak at 1064.5 cm^{-1}attributed to C-O, the bands at 1402 cm^{-1}, 883 cm^{-1} and 1233 cm^{-1} proves the presence of C-H bond representing alkanes, alkenes or aromatic compound, and primary alcohol stretching at 883 cm^{-1} and small band found at 655.6 cm^{-1} and 546 cm^{-1} indicating the presence of C-Cl (Nandiyanto et al., 2022). The result achieved were similar to the work done by Wu & Bao, in the year 2023 and with Garba et al., in the year 2019. From Figure 5(a), surface characteristics of KOH ACDC after adsorption showing a medium band at 3760 cm^{-1} indicating the presence of a free -OH group, stretching of C=O found at 1800 cm^{-1} attributes to the presence of carbonyl group, presence of C=C stretching at 1519 cm^{-1} (alkene or aromatic compound present). At 1018.2, a broad medium peak due stretching of C-N indicating the presence of amines. From Figure 5(b), surface characteristics of $ZnCl_2$ ACDC after adsorption showing a broad stretching at 3035.4 cm^{-1} suggesting the presence C-H stretching, C=O bonds (peak at 1554.7 cm^{-1}), and carbonyl group attributed to the peak at 1031.7 cm^{-1}. The reduction in bands after adsorption is caused due the binding of adsorbate to the surface of the ACDC.

3.5.3. Field Emission Scanning Electron Microscopy (FESEM)

Figures 6(a) and 6(b) shows the SEM image of $ZnCl_2$ activated cow dung carbon, which is found to have a surface morphology, characterized by network of interconnected micropores and macropores. These pores exhibit a broad range of sizes and shapes, which has some macropores interspersed along with micropores contributing to a highly porous structure with increased complexity. The surface texture appears to be rugged and undulating compared to the KOH ACDC, reflecting the action of $ZnCl_2$ and development of micropores and macropores during the activation process.

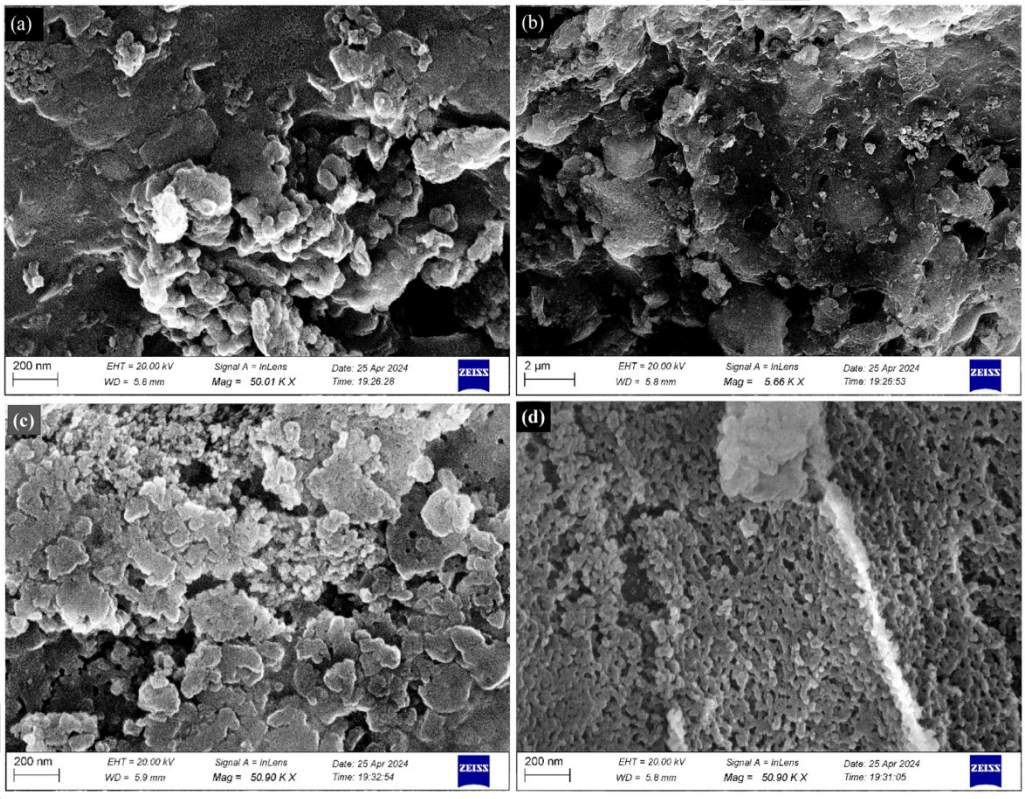

Figure 6. (a) SEM images of $ZnCl_2$ activated cow dung carbon before adsorption (b) SEM images of $ZnCl_2$ activated cow dung carbon before adsorption (c) SEM images of KOH activated cow dung carbon before adsorption and (d) SEM images of KOH activated cow dung carbon before adsorption

Figures 6(c) & 6(d) shows the SEM image of KOH ACDC, the surface morphology shows a finely textured structure characterized by a number of micropores scattered evenly across the sample. Some pores exhibit a uniform size and shape, suggesting controlled activation facilitated by the KOH activation. The surface appears rugged yet well-defined, indicative of the formation of a porous network by the activation process. The presence of such unique surface indicates a porous carbon material with enhanced surface area. Figures 7(a) & 7(b) shows the SEM image of $ZnCl_2$ ACDC after the adsorption process. This picture clearly shows the adsorbent adsorbed to the surface of the ACDC.

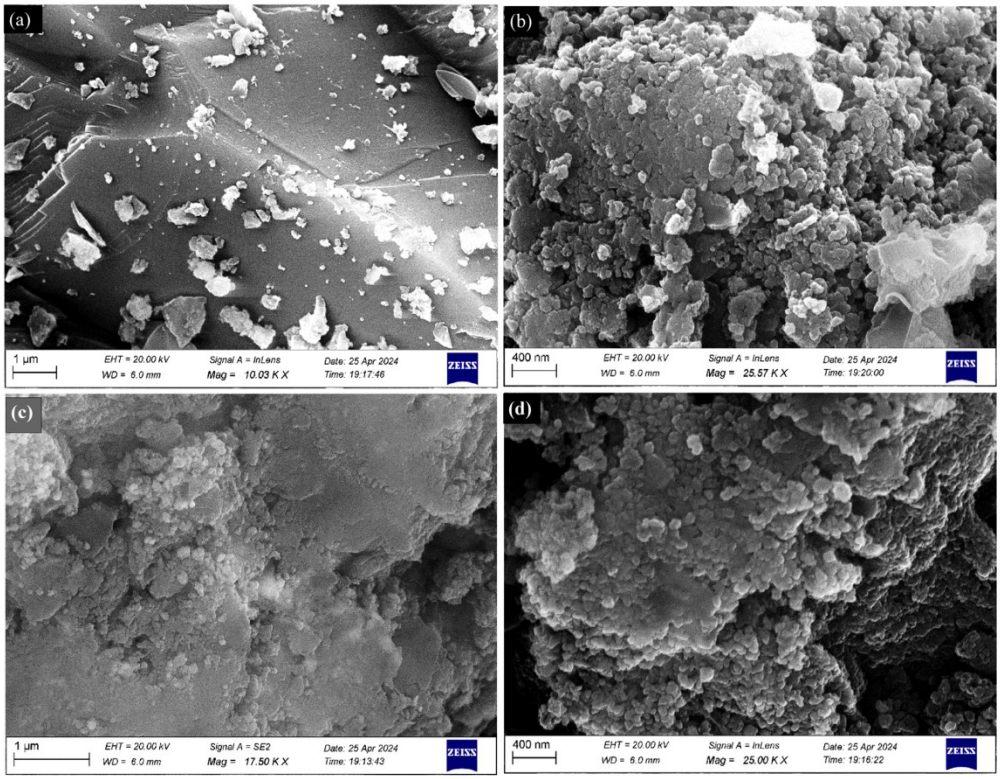

Figure 7. (a) SEM images of $ZnCl_2$ activated cow dung carbon after adsorption (b) SEM images of $ZnCl_2$ activated cow dung carbon after adsorption (c) SEM images of KOH activated cow dung carbon after adsorption and (d) SEM images of KOH activated cow dung carbon after adsorption

Figures 7(c) & 7(d) represents the image of KOH ACDC after adsorption process showing less micropores and very less micropores availability indicating the accumulation of the adsorbate onto the ACDC pores, resulting in the maximum adsorption process. In $ZnCl_2$ ACDC the interconnected mature of the pore network suggests enhanced accessibility and diffusion pathways potentially leading to improved adsorption kinetics and efficiency (Joshiba et al., 2019).

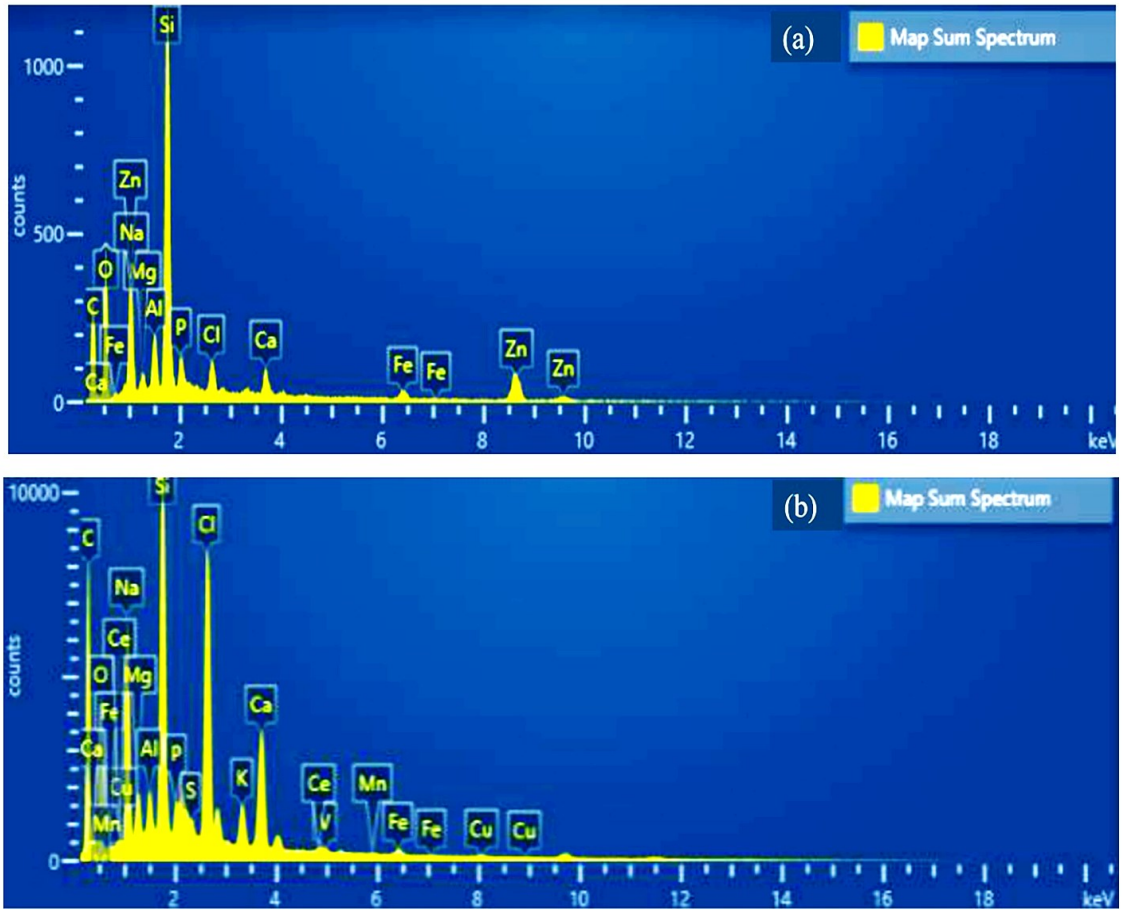

Figure 8. (a) EDX result of $ZnCl_2$ activated cow dung carbon after adsorption studies and (b) EDX result of KOH activated cow dung carbon after adsorption studies

EDX (Energy Dispersive X-ray) gives a quick and nondestructive analysis on the sample's elemental composition is shown in Figure 8. By Table 4, we can infer that the carbon is the

major element of both the ACDC and the presence of silica in high weight percent when compared to other adsorbed elements is due to the precursor materials nature (Li et al., 2018).

Table 4. Weight percent of elements present in KOH and ZnCl2 ACDC after adsorption process by EDX interpretation

Spectrum	**Weight %**	
Elements	**$ZnCl_2$ ACDC**	**KOH ACDC**
C	45.69	58.02
O	25.94	19.82
Na	1.11	4.86
Mg	0.66	0.77
Al	1.74	0.63
Si	11.34	5.07
P	1.13	0.22
Cl	1.21	5.22
Ca	1.17	3.03
Fe	1.12	0.41
Zn	8.88	-
Mn	-	0.09
K	-	0.95
Cu	-	0.25

The diffraction pattern for the sample B-ACK reveals several peaks indicating the presence of various crystalline phases as shown in Figure 9.

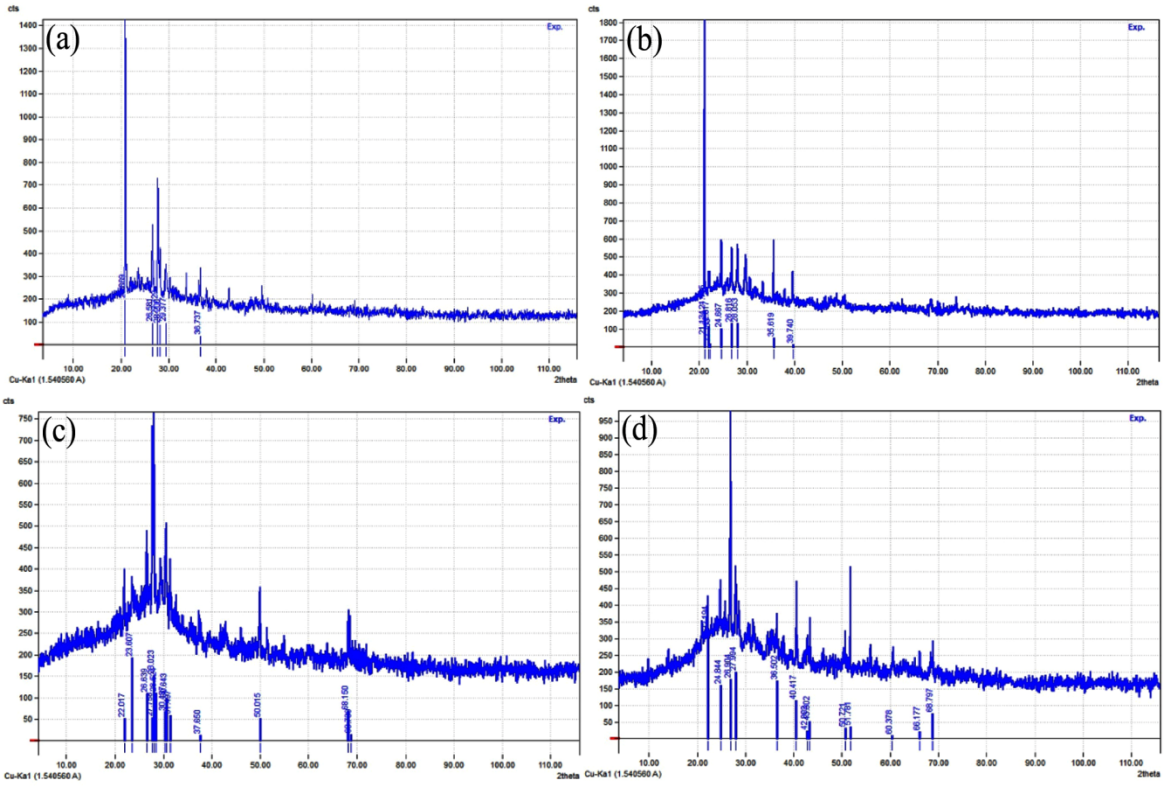

Figure 9. (a) XRD result of KOH activated cow dung carbon after adsorption studies (b) XRD result of $ZnCl_2$ activated cow dung carbon after adsorption studies (c) XRD result of KOH activated cow dung carbon before adsorption studies and (d) XRD result of $ZnCl_2$ activated cow dung carbon before adsorption studies

Key observations are most significant peak was found to be 20.87° 2θ with an intensity of ~1400 counts with other notable peaks were 26.58°, 27.73°, 28.20°, 39.29°, 36.74°. These peaks aid in identifying the phases and their relative abundances within the sample. The lack of Rietveld refinement convergence and the absence of background and alpha2 subtraction may impact the accuracy of integrated profile areas and peak residuals. For the B-ACZ sample, the analysis shows several significant peaks with highest intensity peak to be 2θ = 21.13° corresponding to a d-spacing of 4.201 Å. Overall diffraction profile was dominated by background radiation (88.49%) with diffraction peaks contributing 11.57%. Peak intensity data: 92.54% of peaks

belong to selected phases, with 15.36% unidentified. These peaks indicate multiple crystalline phases, with a need for further refinement to improve data accuracy and phase identification. The diffraction pattern for sample CDK highlights prominent peaks at various 2θ angles with highest intensity peak: Around 27.76°. This pattern is crucial for identifying crystalline phases based on peak positions and intensities. The CDZ sample diffraction pattern shows significant peaks at different 2θ angles with Highest intensity peak: Around 26.90°. This pattern assists in identifying the crystalline phases within the sample.

3.6. COLUMN ADSORPTION STUDY

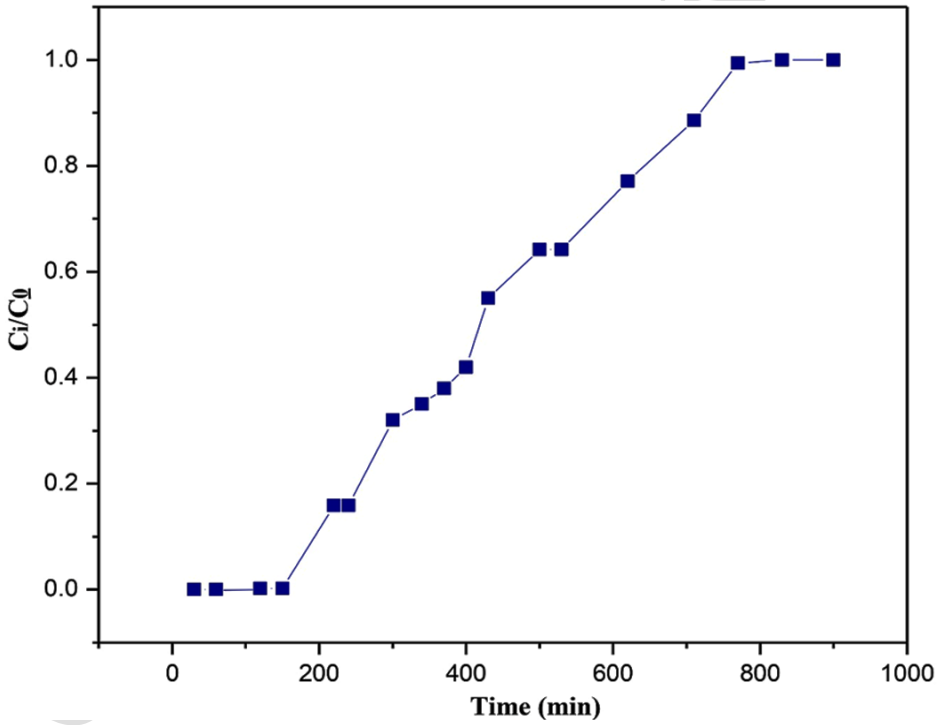

Figure 10. t vs Ci/C0 plot obtained from column study

Considering that the column adsorption process starts with a clean bed with no adsorbent adsorbate on its surface. The introduction of a fresh feed to the column initiates mass transfer of adsorbate from liquid phase to the solid phase, leading to a reduction in adsorbate concentration of treated SDW throughout the bed until it approaches near-zero levels. Feed is continuously

introduced into the column resulting in continuous exposure of the first area of the bed to SDW concentration. As the process goes on the bed eventually attains equilibrium with the feed, resulting in no further mass transfer. This step leads to the channeling effect.

As the SDW reaches the portion of the bed which doesn't attain equilibrium, the mass transfer operation starts to continue until it approaches zero. The mass-transfer zone refers to the area at which the concentration changes. As the process progresses, the adsorbed material gradually achieves equilibrium with the feed. Figure 10 shows an increasing steady increase in the final concentration present in the treated SDW. The feed travel reaching a previously unreached area of the bed equilibrium. The mass-transfer zone expands throughout the bed's length, with an increasing percentage till the bed gets exhausted.

Table 5. Result interpretation of Column study

S. No.	Operation Parameters	Data Points
1	Bed Height (cm)	5 cm
2	Flow Rate	5 ml/min
3	Breakthrough time (t_b)	150 mins
4	Bed exhaustion time (t_e)	810 mins
5	Mass Transfer Zone (min) ($\Delta t = t_e - t_b$)	660 mins
6	Stoichiometric time (t*)	480 mins
7	Length of Unused Bed (LUB)	3.44 cm
8	Avg. Volume of SDW treated	4000 ml
9	Avg. Mass of Adsorbate treated	2100 mg

As shown in Figure 10, the concentration of adsorbate in treated effluent is negligible before the breakthrough point and then it starts to increase as the mass-transfer zone reaches the end of the column. Finally, the of the mass-transfer zone approaches to the end the bed, the effluent concentration increases to the concentration as it is in the feed (i.e., $C_i = C_0$). This occurs at the equilibrium time (t_e), when the whole bed is in equilibrium with the feed. The mid Time of the equilibrium time and the bed saturation time is known as the Stoichiometric time (t*) i.e., the midpoint of the S – shaped curve. Table 5 represents the data obtained from column study including volume treated.

4. CONCLUSION

The following conclusions were observed from the study of cow dung activated carbon as a precursor for synthetic dairy wastewater treatment:

- The batch adsorption investigation demonstrated the efficacy of both $ZnCl_2$ and KOH-treated ACDC in reducing significant SDW parameters, including turbidity. Nevertheless, $ZnCl_2$ ACDC demonstrated a slightly higher level of performance in comparison to KOH ACDC under different conditions. The most effective adsorption was observed when using a dosage of 2.5 g/50 ml.
- $ZnCl_2$ ACDC demonstrated superior performance at an acidic pH of 4, whereas KOH ACDC performed better at a basic pH of 8. Temperature analyses revealed that the adsorption process was more effective at lower temperatures, especially around 30 °C. In addition, the necessary contact time for efficient adsorption was considerably less for $ZnCl_2$ ACDC (10 minutes) in comparison to KOH ACDC (40 minutes).
- The adsorption isotherms and kinetics further corroborated the findings. The Langmuir isotherm model, which accurately characterized $ZnCl_2$ and KOH ACDC adsorption

processes, demonstrated monolayer adsorption with strong correlation coefficients. The adsorption capacity of $ZnCl_2$ ACDC (0.3 mg/g) was much greater than that of KOH ACDC (0.07 mg/g). The data analysis indicated that the pseudo-second-order kinetic model provided the best match.

- The column study demonstrates effective adsorption performance, with the bed efficiently treating synthetic dairy wastewater over a significant duration. The breakthrough time of 150 minutes and exhaustion time of 810 minutes indicate substantial treatment capacity. However, a portion of the adsorbent bed (3.44 cm) remained unused, suggesting potential for optimizing operational parameters such as bed height and flow rate. Despite this, the setup successfully treated 4000 ml of wastewater, removing 2100 mg of contaminants. Further optimization could enhance the efficiency and utilization of the adsorbent.
- Using Raman spectroscopy to characterize the activated carbon showed that its structure changed during adsorption, which suggests that it was able to effectively capture pollutants.
- In summary, the study highlights the efficiency and long-term viability of activated carbon obtained from cow dung as a substance that attracts and holds onto particles in dairy wastewater treatment. The use of $ZnCl_2$ activation is found to offer better results compared to others.

REFERENCES

Ahmad T., Aadil R. M., Ahmed H., Rahman U. U., Soares B. C., Souza S. L., Pimentel T. C., Scudino, H., Guimarães J. T., Esmerino E. A., Freitas M. Q., Almada R. B., Vendramel S. M., Silva M. C., & Cruz A. G. (2019), Treatment and utilization of dairy industrial

waste: A review. *Trends in Food Science & Technology*, **88**, 361–372. https://doi.org/10.1016/j.tifs.2019.04.003.

Basic Animal Husbandry Statistics, Department of Animal Husbandry Dairying & Fisheries, 2023.

Chowdhury S., Misra R., Kushwaha P., & Das P. (2011), Optimum Sorption Isotherm by Linear and Nonlinear Methods for Safranin onto Alkali-Treated Rice Husk. *Bioremediation Journal*, **15(2)**, 77–89. https://doi.org/10.1080/10889868.2011.570282.

Demiral H., & Demiral İ. (2008), Surface properties of activated carbon prepared from wastes. *Surface and Interface Analysis*, **40(3–4)**, 612–615. https://doi.org/10.1002/sia.2716.

Dubey P., Shrivastav V., Gupta B., Hołdyński M., Nogala W., & Sundriyal S. (2022), Diffusion and surface charge studies of waste cow dung derived highly porous carbon as a facile electrode for solid-state supercapacitors. *Diamond and Related Materials*, **130**, 109529. https://doi.org/10.1016/j.diamond.2022.109529.

Fdegaard H., & Rusten B. (1980), Nitrogen removal in rotating biological contactors without the use of external carbon source. *Kankyō Gijutsu/Kankyou Gijutsu*, **9(6)**, 493–498. https://doi.org/10.5956/jriet.9.493.

Food and Agriculture Organization of the United Nations - report, 2023.

Garba J., Samsuri W. A., Othman R., & Hamdani M. S. A. (2019), Evaluation of adsorptive characteristics of cow dung and rice husk ash for removal of aqueous glyphosate and aminomethylphoshonic acid. *Scientific Reports*, **9(1)**.

Healy M., Rodgers M., & Mulqueen J. (2007), Performance of a stratified sand filter in removal of chemical oxygen demand, total suspended solids and ammonia nitrogen from high-

strength wastewaters. *Journal of Environmental Management*, **83(4)**, 409–415. https://doi.org/10.1016/j.jenvman.2006.03.005.

Joshiba G. J., Kumar P. S., Femina C. C., Jayashree E., Racchana R., & Sivanesan S. (2019), Critical review on biological treatment strategies of dairy wastewater. *DESALINATION AND WATER TREATMENT*, **160**, 94–109. https://doi.org/10.5004/dwt.2019.24194.

Kulkarni R. M., Dhanyashree J., Varma E., & Sirivibha S. (2022), Batch and continuous packed bed column studies on biosorption of nickel (II) by sugarcane bagasse. *Results in Chemistry*, **4**, 100328. https://doi.org/10.1016/j.rechem.2022.100328.

Kushwaha J. P., Srivastava V. C., & Mall I. D. (2010), Treatment of dairy wastewater by inorganic coagulants: Parametric and disposal studies. *Water Research*, **44(20)**, 5867–5874. https://doi.org/10.1016/j.watres.2010.07.001.

Li H., Yang S., Sun H., & Liu X. (2018), Production of Activated Carbon from Cow Manure for Wastewater Treatment. *Bioresources*, **13(2)**.

Liu Y., Liu X., Dong W., Zhang L., Kong Q., & Wang W. (2017), Efficient Adsorption of Sulfamethazine onto Modified Activated Carbon: A Plausible Adsorption Mechanism. *Scientific Reports*, **7(1)**. https://doi.org/10.1038/s41598-017-12805-6.

Luo J., & Ding L. (2011), Influence of pH on treatment of dairy wastewater by nanofiltration using shear-enhanced filtration system. *Desalination*, **278(1–3)**, 150–156. https://doi.org/10.1016/j.desal.2011.05.025.

Mucha Z., & Kułakowski P. (2016), Turbidity measurements as a tool of monitoring and control of the SBR effluent at the small wastewater treatment plant – preliminary study. *Archives of Environmental Protection*, **42(3)**, 33–36. https://doi.org/10.1515/aep-2016-0030.

Muniz G. L., Da Silva T. C. F., & Borges A. C. (2020), Assessment and optimization of the use of a novel natural coagulant (Guazuma ulmifolia) for dairy wastewater treatment. *Science of the Total Environment*, **744**, 140864. https://doi.org/10.1016/j.scitotenv.2020.140864.

Nandiyanto A. B. D., Ragadhita R., & Fiandini M. (2022), Interpretation of fourier Transform Infrared Spectra (FTIR): a practical approach in the Polymer/Plastic thermal decomposition. *Indonesian Journal of Science and Technology*, **8(1)**, 113–126. https://doi.org/10.17509/ijost.v8i1.53297.

Özcan A., & Özcan A. (2004), Adsorption of acid dyes from aqueous solutions onto acid-activated bentonite. *Journal of Colloid and Interface Science*, **276(1)**, 39–46. https://doi.org/10.1016/j.jcis.2004.03.043.

Park J. E., Lee G. B., Kim H., & Hong B. U. (2022), High Surface Area–Activated Carbon Production from Cow Manure Controlled by Heat Treatment Conditions. *Processes*, **10(7)**, 1282. https://doi.org/10.3390/pr10071282.

Pathak U., Das P., Banerjee P., & Datta S. (2016), Treatment of Wastewater from a Dairy Industry Using Rice Husk as Adsorbent: Treatment Efficiency, Isotherm, Thermodynamics, and Kinetics Modelling. *Journal of Thermodynamics*, 1–7. https://doi.org/10.1155/2016/3746316.

Ramya M. R., Likith Kumar N., Ravichandra, Tejas R., & Vinutha R. (2021), REMOVAL OF TURBIDITY FROM DAIRY WASTEWATER USING NATURAL COAGULANTS IN COMBINATION. *International Research Journal of Engineering and Technology (IRJET)*, **08(09)**, 2395–0056.

Rosa D. R., Duarte I. C., Saavedra N. K., Varesche M. B., Zaiat M., Cammarota M. C., & Freire D. M. (2009), Performance and molecular evaluation of an anaerobic system with

suspended biomass for treating wastewater with high fat content after enzymatic hydrolysis. *Bioresource Technology*, **100(24)**, 6170–6176. https://doi.org/10.1016/j.biortech.2009.06.089.

Santos A. D., Martins R. C., Quinta-Ferreira R. M., & Castro L. M. (2020), Moving bed biofilm reactor (MBBR) for dairy wastewater treatment. *Energy Reports*, **6**, 340–344. https://doi.org/10.1016/j.egyr.2020.11.158.

Shete B. S., & Shinkar N. P. (2013), Dairy Industry Wastewater Sources, Characteristics & its Effects on Environment. *International Journal of Current Engineering and Technology*.

Slavov A. K. (2017), Dairy Wastewaters – General Characteristics and Treatment Possibilities – A review. *Food Technology and Biotechnology*, **55(1)**. https://doi.org/10.17113/ftb.55.01.17.4520.

Stanly S., Jelmy E. J., & John H. (2020), Studies on modified Montmorillonite clay and its PVA nanohybrid for water purification. *Journal of Polymers and the Environment*, **28(9)**, 2433–2443. https://doi.org/10.1007/s10924-020-01786-9.

Tikariha A., & Sahu O. (2014), Study of Characteristics and Treatments of Dairy Industry Waste water. *Journal of Applied & Environmental Microbiology*, **2(1)**, 16–22. https://doi.org/10.12691/jaem-2-1-4.

Vourch M., Balannec B., Chaufer B., & Dorange G. (2008), Treatment of dairy industry wastewater by reverse osmosis for water reuse. *Desalination*, **219(1–3)**, 190–202. https://doi.org/10.1016/j.desal.2007.05.013.

Yonar T., Sivrioğlu Ö., & Özengin N. (2018), Physico-Chemical Treatment of Dairy Industry Wastewaters: A review. *Technological Approaches for Novel Applications in Dairy Processing*. https://doi.org/10.5772/intechopen.77110.

List of Table captions:

Table 1. Composition of SDW

Table 2. Adsorption isotherm parameters of ZnCl2 ACDC & KOH ACDC

Table 3. Parameter analysis of synthetic dairy water with before and after ZnCl2 and KOH ACDC treatment at optimum condition

Table 4. Weight percent of elements present in KOH and ZnCl2 ACDC after adsorption process by EDX interpretation

Table 5. Result interpretation of Column study

List of Figure captions:

Figure 1. (a) Adsorbent Dosage optimization graph for both ACDC (b) pH optimization graph for both ACDC (c) Temperature optimization graph for both ACDC and (d) Time optimization graph for both ACDC

Figure 2. (a) Langmuir isotherm of ZnCl2 ACDC (b) Freundlich isotherm of ZnCl2 ACDC (c) Langmuir isotherm of KOH ACDC and (d) Freundlich isotherm of KOH ACDC

Figure 3. (a) Pseudo 1st order kinetics of ZnCl2 ACDC (b) Pseudo 2st order kinetics of ZnCl2 ACDC (c) Pseudo 1st order kinetics of KOH ACDC and (d) Pseudo 2nd order kinetics of KOH ACDC

Figure 4. (a) Raman spectra of ZnCl2 ACDC activated carbon before and after adsorption and (b) Raman spectra of KOH ACDC activated carbon before and after adsorption

Figure 5. (a) FTIR of ACDC KOH activated carbon before and after adsorption and (b) FTIR of ACDC ZnCl2 activated carbon before and after adsorption

Figure 6. (a) SEM images of ZnCl2 activated cow dung carbon before adsorption (b) SEM images of ZnCl2 activated cow dung carbon before adsorption (c) SEM images of KOH activated cow dung carbon before adsorption and (d) SEM images of KOH activated cow dung carbon before adsorption

Figure 7. (a) SEM images of ZnCl2 activated cow dung carbon after adsorption (b) SEM images of ZnCl2 activated cow dung carbon after adsorption (c) SEM images of KOH activated cow dung carbon after adsorption and (d) SEM images of KOH activated cow dung carbon after adsorption

Figure 8. (a) EDX result of ZnCl2 activated cow dung carbon after adsorption studies and (b) EDX result of KOH activated cow dung carbon after adsorption studies

Figure 9. (a) XRD result of KOH activated cow dung carbon after adsorption studies (b) XRD result of ZnCl2 activated cow dung carbon after adsorption studies (c) XRD result of KOH activated cow dung carbon before adsorption studies and (d) XRD result of ZnCl2 activated cow dung carbon before adsorption studies

Figure 10. t vs Ci/C0 plot obtained from column study